INTERNATIONAL ATOMIC ENERGY AGENCY
UNITED NATIONS EDUCATIONAL, SCIENTIFIC AND CULTURAL ORGANIZATION

INTERNATIONAL CENTRE FOR THEORETICAL PHYSICS
34100 TRIESTE (ITALY) - P.O.B. 586 - MIRAMARE - STRADA COSTIERA 11 - TELEPHONE: 2240-1
CABLE: CENTRATOM - TELEX 460392-1

SMR/291 - 47

SPRING COLLEGE IN CONDENSED MATTER
ON
"THE INTERACTION OF ATOMS & MOLECULES WITH SOLID SURFACES"
(25 April - 17 June 1988)

REACTIONS ON SURFACES AND CATALYSIS
(Lectures IV & V)

David W. GOODMAN
Surface Science Division
Sandia National Laboratories
Albuquerque, New Mexico 87185
U.S.A.

Reactivity of Chemically Modified Surfaces

D. W. Goodman
Surface Science Division
Sandia National Laboratories
Albuquerque, NM 87185

ABSTRACT

Several reactions representing important categories of catalytic systems have been studied on chemically modified single crystal surfaces of Ni, Ru, and Rh. These reactions are the methanation of CO and CO_2, the hydrogenolysis of ethane, and cyclopropane ring-opening and hydrogenolysis. Poisoning of the above reactions by ordered, submonolayer coverages of sulfur show large nonlinear effects for the attenuation of reactivity versus sulfur coverage. Similar studies have addressed the role of potassium promoters in CO and CO hydrogenation reactions. These data, together with related chemisorption results, are reviewed with an emphasis on the author's and collaborators' work.

It has long been recognized that the addition of impurities to metal catalysts can produce large effects on the activity, selectivity, and resistance to poisoning of the pure metal [1]. For example, the catalytic properties of metals can be altered greatly by the addition of a second transition or group 1B metal or by the addition of impurities such as potassium or sulfur. On the other hand, catalytic processing is often plagued by loss of activity and/or selectivity due to the inadvertent contamination of catalysts by undesirable impurities. Although these effects are well recognized in the catalytic industry, the mechanisms responsible for surface chemical changes induced by surface additives are poorly understood. However, the current interest and activity in this area of research promises a better understanding of the fundamentals by which impurities alter surface chemistry.

A pivotal question concerns the underlying relative importance of ensemble (steric or local) versus electronic (nonlocal or extended) effects. A general answer to this question will critically influence the degree to which we will ultimately be able to tailor-make exceptionally efficient catalysts by fine tuning the electronic structure. If, indeed, low concentrations of surface impurity can profoundly alter the surface electronic structure and thus catalytic activity, then the possibilities for the systematic manipulation of these properties via the selection of the appropriate additive would appear limitless. On the other hand, if steric effects dominate the mode by which surface additives alter the catalytic chemistry, then a different set of considerations for catalyst

alteration come into play, a set which will most certainly be more constraining than the former. In the final analysis, a complete understanding will include components of both electronic and ensemble effects, the relative importance of each to be assessed for a given reaction and conditions. A major emphasis of our research has been in the area of addressing and partitioning the importance of these two effects in the influence of surface additives in catalysis.

Catalyst deactivation and promotion are extremely difficult questions to address experimentally [1]. For example, the interpretation of related data on dispersed catalysts is severely limited by the uncertainty concerning the structural characterization of the active surface. Specific surface areas cannot always be determined with adequate precision. In addition, a knowledge of the crystallographic orientation, the concentration and the distribution of impurity atoms, as well as their electronic states is generally poor. The degree of contamination may vary considerably along the catalytic bed and the impurity very well may alter the support as well as the metal. Moreover, the active surface may be altered in an uncontrolled manner as a result of sintering or faceting during the reaction itself.

The use of metal single crystals in catalytic reaction studies essentially eliminates the difficulties mentioned above and allows, to a large extent, the utilization of a homogeneous surface amenable to study using modern surface analytical techniques. Carefully prepared, single-crystal catalytic

surfaces are particularly suited to the study of impurity effects on catalytic behavior because of the ease with which impurity atoms can be uniformly introduced to the surface. Although the studies to date are few, the results appear quite promising in addressing the fundamental aspects of catalytic poisoning and promotion.

These studies were carried out utilizing the specialized apparatus described in references [2,3]. This device consists of two distinct regions, a surface analysis chamber and a microcatalytic reactor. The custom built reactor, contiguous to the surface analysis chamber, employs a retraction bellows that supports the metal single crystal and allows translation of the catalyst in vacuo from the reactor to the surface analysis region. Both regions are of ultrahigh vacuum construction, bakeable, and capable of ultimate pressures of less than 2×10^{-10} Torr. Auger spectroscopy (AES) is used to characterize the sample before and after reaction. A second chamber was equipped with Auger spectroscopy, low energy electron diffraction (LEED) and a mass spectrometer for temperature programmed desorption (TPD).

Impurities whose electronegativities are greater than those for transition metals generally poison a variety of catalytic reactions, particularly those involving H_2 and CO. Of these poisons sulfur is the best known and technologically the most important [1]. The first step in the systematic definition of the poisoning mechanism of this category of impurities is the study of the influence of these impurities on the adsorption and desorption of the reactants.

The effect of preadsorbed electronegative atoms Cl, S, and P on the adsorption-desorption of CO and H_2 on Ni(100) has been extensively studied [4-11] using temperature programmed desorption, low energy electron diffraction, and Auger spectroscopy. It has been found that the presence of the electronegative atoms Cl, S, and P, causes a reduction of the sticking coefficient, the adsorption bond strength, and the adsorption capacity of the Ni(100) surface for CO and H_2. Furthermore, the poisoning effect becomes more prominent with increasing electronegativity of the preadsorbed atoms [12].

Figures 1 and 2 show the observed dependence of the total H_2 and CO adsorption on the coverage of Cl, S, and P. Coverages of impurities are expressed in terms of monolayers, ML, or the ratio of surface impurity atoms to the surface metal atoms. The data represent the total H_2 and CO desorption, as determined by TPD, for different impurity coverages after an exposure sufficient to reach the saturation adsorbate coverage. Both CO and H_2 adsorption decrease markedly in the presence of surface impurities. The effects of P, however, are much less pronounced than for Cl or S. As seen in Fig. 1, the reduction of H_2 coverage is most apparent in the presence of Cl atoms. The similarity in the atomic radii of Cl, S, and P (0.99, 1.04, and 1.10A, respectively [13]) suggests a relationship between electronegativity and the poisoning of chemisorptive properties by these surface impurities. Related studies [6] have been carried out in the presence of C and N. These impurities have the same electronegativities as S and Cl, 2.5 and 3.0, respectively.

The comparison between the results for C and N and those for S and Cl are entirely consistent with the interpretation that electronegativity effects dominate the poisoning of chemisorption by surface impurities with similar atomic size, and which occupy the same adsorption sites. In the case of adsorbed impurities with the same electronegativity, but with different atomic radii (S and C, Cl and N), the effect becomes less pronounced with decreasing atomic radius.

Particularly noteworthy in the above studies is the general observation that those impurities strongly electronegative with respect to nickel, e.g. Cl, N, and S, modify the chemisorptive behavior far more strongly than would result from a simple site blocking model. The initial effects of these impurities as shown in Figs. 1 and 2 suggest that a single impurity atom can successfully poison more than just its four nearest neighbor nickel atoms. This effect is especially apparent for hydrogen adsorption on the sulfur covered Ni(100) surface. Poisoning of next nearest neighbors supports an interaction that is primarily electronic in nature.

Kinetic studies have been carried out for several reactions as a function of sulfur coverage over single crystals of nickel [4] rhodium [14], and ruthenium [15]. For the methanation reaction over Ni(100) [4], the sulfided surface (Fig. 3a) shows behavior remarkably similar to results for the clean surface at a considerably reduced hydrogen partial pressure. For clean Ni(100) [16] a departure from Arrhenius linearity is observed at 700K. Associated with the onset of this nonlinearity or "rollover" is a rise in the surface carbon level. This rise in

carbon level continues until the carbon level reaches 0.5 ML, i.e. the saturation level. This behavior of the Arrhenius plot has been interpreted [16] as reflecting the departure of atomically adsorbed hydrogen from a saturation or critical coverage. For a sulfur surface coverage of 4% the reaction rate at identical conditions departs similarly from linearity at 600K, some 100K lower in reaction temperature. Here too, an increase in surface carbon level is associated with this deviation from linearity. This behavior indicates that the sulfur is very effective in reducing the steady-state surface atomic hydrogen coverage which results in an attenuation of the rate of surface carbon hydrogenation. These results are consistent with the chemisorption results [5] discussed above for H_2 on sulfur poisoned Ni(100) surface. Similar results (Fig. 9b) have been seen [15] for sulfur poisoning of a Ru(0001) surface toward CO hydrogenation.

Both the kinetics and the TPD studies show that the poisoning effects of sulfur are very nonlinear. Figure 4a shows the relationship found between the sulfur coverage on Ni(100), Rh(100), and Ru(0001) catalysts and the methanation rate catalyzed by these surfaces at 600K. A precipitous drop in the catalytic activity is observed for low sulfur coverages. The poisoning effect quickly maximizes with little reduction in the reaction rate at sulfur coverages exceeding 0.2 monolayers. The activity attenuation at the higher sulfur coverages on nickel is in excellent agreement with that found for supported Ni/Al_2O_3 by Rostrup-Nielsen and Pedersen [17]. The initial changes in the

rates in Fig. 4a-c suggest that more than ten metal atom sites are deactivated by one sulfur atom.

In those cases where multiple products are possible, dramatic modifications in the selectivity, or distributions of these products, have been observed [18]. Figure 5 shows the effect that progressive sulfiding of a Ni(111) catalyst has on the cyclopropane/hydrogen reaction. A small amount of sulfur (<0.1 ML) exponentially lowers the rate of methane formation, the dominant product formed on the clean surface. Similarly, the rate of ethane formation falls in concert with the methane suggesting, as is expected, a close correlation between these hydrogenolysis products. In contrast to the methane and ethane products, the production of propane/propylene (C_3) product actually increases with the sulfur addition. Qualitatively, the increase in the C_3 product corresponds to the decrease in the methane rate. These results show rather directly that the initial sulfiding promotes the ring-opening reaction by reducing the tendency of the surface to break more than one carbon-carbon bond.

In contrast to the clean Ni(111) surface where no ethylene was observed as a reaction product, significant amounts of ethylene are found [18] for the sulfided surface. In addition to reducing the tendency of the surface to break carbon-carbon bonds, sulfur also lowers the hydrogenation activity. This tendency has been confirmed by measuring directly the attenuation of the hydrogenative character of Ni(111) versus sulfur coverage by monitoring the ethylene/hydrogenative reaction [19].

At first glance one might interpret these results as the

simple poisoning of minority or defect sites on the surface and that these sites are crucial to the reactivity at steady-state reaction conditions and the TPD decomposition. However, this is a very unlikely explanation given the close correspondence between the steady-state rates measured for single crystal catalysts and those rates found for supported, small-particle catalysts seen in Section 3.1. That the defect densities on these two very different materials would be precisely the same is highly unlikely. It is much more likely that these reactions are not defect controlled and that the surface atoms of the single crystals are uniformly active. There are two other possible explanations for this result: (1) an electronic or ligand effect or (2) an ensemble effect, the requirement that a certain collection of surface atoms are necessary for the reaction to occur. Experimentally these two possibilities can be distinguished [7,20]. If an ensemble of more than ten nickel atoms is required for methanation, then altering the electronic character of the impurity should produce little change in the degree to which the impurity poisons the catalytic activity. That is, the impurity serves merely to block a single site in the reaction ensemble, nothing more. On the other hand, if electronic effects are playing a significant role in the poisoning mechanism, then the reaction rate should respond to a change in the electronic character of the impurity. Substituting phosphorus for sulfur (both atoms are approximately the same size) in a similar set of experiments results in a marked change in the magnitude of poisoning at low coverages as shown in Figure

6. Phosphorus, because of its less electronegative character, effectively poisons only the four nearest neighbor metal atom sites.

Effective poisoning of catalytic activity at sulfur coverages less than 0.1ML has been observed for other reactions including ethane and cyclopropane hydrogenolysis [18], ethylene hydrogenation [19], and CO_2 methanation [21]. The results of several studies on nickel are summarized in Figure 7. These studies indicate that the sensitivity of the above reactions to sulfur poisoning are generally less than that for poisoning by sulfur of CO methanation. The rate attenuation is, nevertheless, strongly nonlinear at the lower sulfur levels. A direct consequence of the differing molecular sizes of the reactants (CO, ethylene, ethane, cyclopropane) involved in the reactions investigated is that electronic effects, rather than ensemble requirements, dominate the catalytic poisoning mechanism for these experimental conditions.

Recent studies [22] using high resolution electron energy loss and photoelectron spectroscopy to investigate the effect of sulfur on the CO/Ni(100) system are consistent with an extended effect by the impurity on the adsorption and bonding of CO. Sulfur levels of a few percent of the surface nickel atom concentration were found sufficient to significantly alter the surface electronic structure as well as the CO bond strength.

A direct consequence of interpreting the poisoning effects of electronegative impurities in terms of electronic surface modification is that additives with electronegativities less than that of the metal should promote a different chemistry reflecting

the donor nature of the additive. For example, alkali atoms on a transition metal surface are known to exist in a partially ionic state, donating a large fraction of their valence electron to the metal, resulting in a work function decrease. This additional electron density on the transition metal surface atoms is thought to be a major factor in alkali atoms altering the chemisorptive bonding of molecules such as N_2 [23] or CO [24], and in promoting the catalytic activity in ammonia synthesis [25]. These results are consistent with the general picture that electron acceptors tend to inhibit CO hydrogenation reactions whereas electron donors typically produce desirable catalytic effects, including increased activity and selectivity. Recent chemisorption and kinetic studies have examined quantitatively the relationship between the electron donor properties of the impurity and its effect on the catalytic behavior.

The addition of alkali metal atoms to Ni(100) results in the appearance of more tightly bound states in the CO TPD spectra and dissociation probability increases in the sequence Na, K, Cs, indicating a correspondence between the donor properties of the impurity and its ability to facilitate CO dissociation. On iron [26], CO adsorbs with a higher binding energy on the potassium promoted Fe(110) surface than on the corresponding clean surface. The CO coverage increases and the sticking coefficient decreases with increasing potassium coverage. The probability for CO dissociation increases in the presence of potassium [26]. Analogously, NO is more strongly adsorbed and dissociated to a greater extent on sodium covered Ag(111) than on clean Ag(111)

[27]. The addition of potassium to iron increases the dissociative adsorption of N_2, isoelectronic with CO, by a factor of 300 over that for the clean surface [28]. Recent studies of CO adsorption on potassium promoted Pt(111) [29-31] and Ni(100) [32] are consistent with this general picture of donor-enhanced metal-CO bonding. For H_2 chemisorption, Ertl and coworkers [33], using TPD techniques, have observed an increase in the adsorption energy of hydrogen on iron. They suggest that the empty state above the Fermi level created by the pronounced electron transfer from potassium to the d-band of iron may possibly be involved via interaction with the H 1s level.

Adsorbed potassium causes a marked increase in the rate of CO dissociation on a Ni(100) catalyst [34]. The increase of the initial formation rate of "active" carbon or carbidic carbon via CO disproportionation is illustrated in Fig. 8. The relative rates of CO dissociation were determined for the clean and potassium covered surfaces by observing the growth in the carbon Auger signal with time in a CO reaction mixture, starting from a carbon-free surface. The rates shown in Fig. 8 are the observed rates of carbon formation extrapolated to zero carbon coverage. Of particular significance in these studies is the reduction of the activation energy of reactive carbon formation from 23 kcal $mole^{-1}$ for the clean Ni(100) surface to 10 kcal $mole_{-1}$ for a 10% potassium covered surface [34].

Kinetic measurements [34] over a Ni(100) catalyst containing well-controlled submonolayer quantities of potassium show a general decrease in the steady-state methanation rate with little apparent change in the activation energy associated with the

kinetics (Fig. 9). However, the potassium did change the steady-state coverage of active carbon on the catalyst. This carbon level changed from 10% of a monolayer on the clean catalyst to 30% on the potassium covered catalyst.

Adsorbed potassium causes a marked increase in the steady-state rate and selectivity of nickel for higher hydrocarbon synthesis [34]. At all temperatures studied, the overall rate of higher hydrocarbon production was faster on the potassium-dosed surface showing that potassium is a promoter with respect to Fischer-Tropsch synthesis. This increase in higher hydrocarbon production is attributed to the increase in the steady-state active carbon level during the reaction, a factor leading to increased carbon polymerization. Potassium impurities on a nickel catalyst, then, cause a significant increase in the CO dissociation rate and a decrease in the activation energy for CO dissociation at low carbon coverages. These effects can be explained in terms of an electronic effect, whereby the electropositive potassium donates extra electron density to the nickel surface atoms, which in turn donate electron density to the adsorbed CO molecule. This increases the extent of pi-backbonding in the metal-CO complex, resulting in an increased metal-CO bond strength and a decrease in C-O bond strength. This model satisfactorily explains the decrease in the activation energy for carbide build-up brought about by potassium.

Intrinsic to interpreting catalytic poisoning and promotion in terms of electronic effects is the inference that adsorption of an electropositive impurity should moderate or compensate for

the effects of an electronegative impurity. Recent experiments have shown this to be true in the case of CO_2 methanation [21] where the adsorption of sulfur decreases the rate of methane formation significantly. The adsorption of potassium in the presence of sulfur indicates that the potassium can neutralize the effects of sulfur.

ACKNOWLEDGEMENT

We acknowledge with pleasure the partial support of this work by the Department of Energy, Office of Basic Energy Sciences, Division of Chemical Sciences.

REFERENCES

1. B. Imelik, C. Naccache, G. Coudurier, H. Praliaud, P. Meriaudeau, P. Gallezot, G. A. Martin, and J. C. Vedrine, (Eds) "Metal-Support and Metal-Additive Effects in Catalysts", Elsevier, 1982.

2. D. W. Goodman, R. D. Kelley, T. E. Madey, and J. T. Yates, Jr., J. Catal. 64, 479 (1980).

3. D. W. Goodman, Ann. Rev. Phys. Chem., 37 (1986) 425; D. W. Goodman, J. Vac. Sci. Tech., 20, 522 (1982).

4. D. W. Goodman and M. Kiskinova, Surf. Sci., 105, L265 (1981).

5. M. Kiskinova and D. W. Goodman, Surf. Sci., 108, 64 (1981).

6. M. Kiskinova and D. W. Goodman, Surf. Sci., 109, L555 (1981).

7. D. W. Goodman, Appl. Surf. Sci., 19, 1 (1984).

8. S. Johnson and R. J. Madix, Surf. Sci., 108, 77 (1981).

9. R. J. Madix, M. Thornburg, and S. -B. Lee, Surf. Sci., 133, L447 (1983).

10. R. J. Madix, S. -B. Lee, and M. Thornburg, J. Vac., Sci. Technol., A1, 1254 (1983).

11. E. L. Hardegree, P. Ho., and J. M. White, to be published.

12. M. Kiskinova and D. W. Goodman, Surf. Sci., 108, 64 (1981).

13. C. Kittel, "Introduction to Solid State Physics", John Wiley & Sons, Inc., New York, 1971.

14. D. W. Goodman in "Heterogeneous Catalysis" (Proceedings of IUCCP Conference), Texas A&M University, 1984.

15. C. H. P. Peden and D. W. Goodman, ACS Symposium Series, Proceedings of Sym. on the Surface Science of Catalysis, Eds. M. L. Devinny and J. L. Gland, Philadelphia, 1984

16. D. W. Goodman, R. D. Kelley, T. E. Madey and J. T. Yates, Jr., J. Catal., 63, 226 (1980).

17. J. R. Rostrup-Nielsen, K. Pedersen, J. Catal., 59, 395 (1979).

18. D. W. Goodman, J. Vac. Sci. Technol., A2, 873 (1984).

19. D. W. Goodman, unpublished results.

20. D. W. Goodman, Accts. Chem. Res., 17, 194 (1984)

21. D. E. Peebles, D. W. Goodman, and J. M. White, J. Phys. Chem., 87, 4378 (1983).

22. J. E. Houston, J. R. Rogers, D. W. Goodman and D. N. Belton, J. Vac. Sci. Technol., A2, 882 (1984).

23. S. Anderson, U. Jostell, Surf. Sci., 46, 625 (1974).

24. M. Kiskinova, Surf. Sci., 111, 584 (1981).

25. G. Ertl, Catalysis Rev.-Sci. Eng., 21, 201 (1980).

26. G. Broden, G. Gafner, and H. P. Bonzel, Surf. Sci., 84, 295 (1979).

27. P. J. Goddard, J. West, and R. M. Lambert, Surf. Sci., 71, 447 (1978).

28. G. Ertl, M. Weiss, and S. B. Lee, Chem. Phys. Lett., 60, 391 (1979).

29. J. E. Crowell, E. L. Garfunkel, and G. A. Somorjai, Surf. Sci., 121, 303 (1982).

30. E. L. Garfunkel, J. E. Crowell, G. A. Somorjai, J. Phys. Chem. 86, 310 (1982).

31. M. P. Kiskinova, G. Pirug, and H. P. Bonzel, Surf. Sci., 140, 1 (1984).

32. H. S. Luftman, Y.-M. Sun, and J. M. White, Appl. Surf. Sci., 19, 59 (1984).

33. G. Ertl, S. B. Lee, and M. Weiss, Surf. Sci., 111, L711 (1981).

34. C. T. Campbell and D. W. Goodman, Surf. Sci., 123, 413 (1982).

Figure 1. Dependence of H_2 coverage on Ni(100) on additive precoverage. (From refs. [4-11])

Figure 2. Dependence of saturation CO coverage on Ni(100) on additive precoverage. (From refs. [4-11])

Figure 3. An Arrhenius plot of the rate of methanation over sulfided (a) Ni(100) [4] and (b) Ru(0001) [15] catalysts at 120 Torr and a H_2/CO ratio of four. Coverages are expressed as fractions of a monolayer. N_{CH4} is the turnover frequency or the number of methane molecules produced per surface nickel atom per second.

Figure 4. Methanation rate as a function of sulfur coverage on a (a) Ni(100) [4], (b) Ru(0001) [15], and (c) Rh(111) [14] catalyst. Pressure = 120 Torr, H_2/CO = 4, Reaction Temperature = 600K.

Figure 5. Product distribution from the reaction of cyclopropane with hydrogen as a function of sulfur coverage over a Ni(111) catalyst. Temperature = 550K. Total pressure = 100 Torr. H_2/cyclopropane = 100. (From ref. [16])

Figure 6. A plot of the rate of CO methanation as a function of sulfur and phosphorous coverage over a Ni(100) catalyst at 120 Torr and a H_2/CO ratio equal to four. (From ref. [16])

Figure 7. Sulfur poisoning of various reactions over nickel. Hydrogen partial pressure = 100 Torr. (From refs. [3])

Figure 8. The relative initial rate of reactive carbon formation from CO disproportionation as a function of potassium coverage. P_{CO} = 24 Torr, T = 500K. (From ref. [34])

Figure 9. A comparison of the rate of methane synthesis over a clean single crystal Ni(100) catalyst with the corresponding rate over a potassium doped catalyst. Total reactant pressure is 120 Torr, H_2/CO = 4/1. (From ref. [34])

Fig. 5

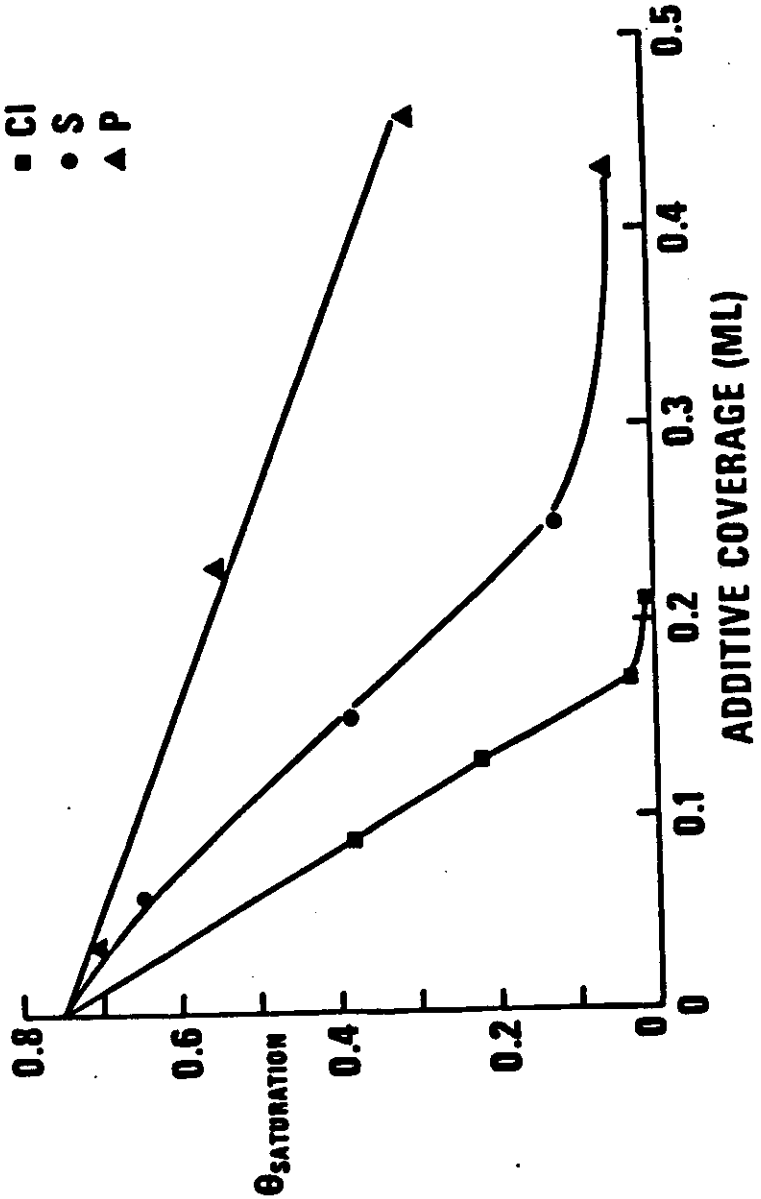

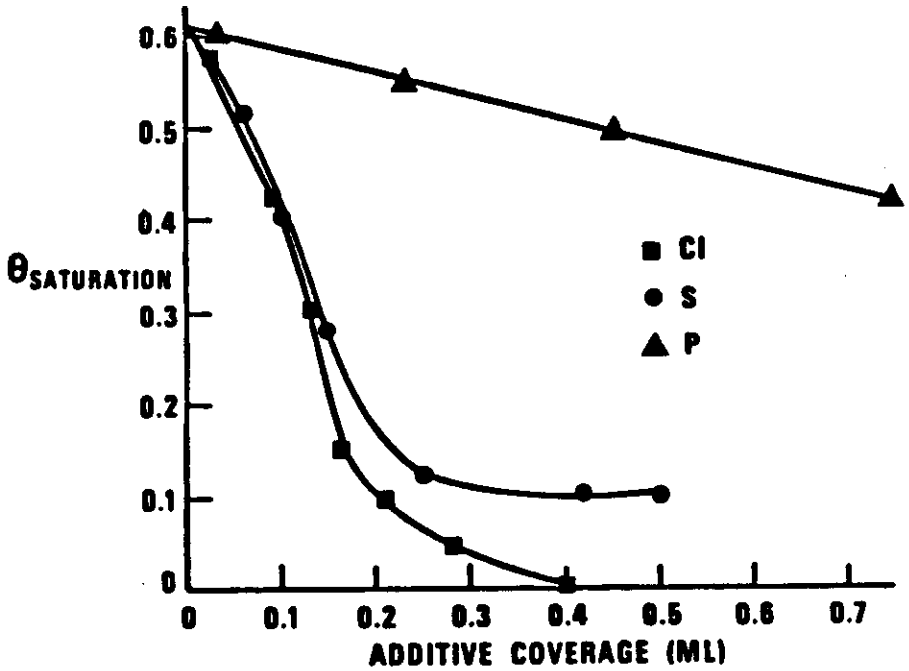
θSATURATION
0.6
0.5
0.4
0.3
0.2
0.1
0
0 0.1 0.2 0.3 0.4 0.5 0.6 0.7
ADDITIVE COVERAGE (ML)
Cl
S
P

(2)

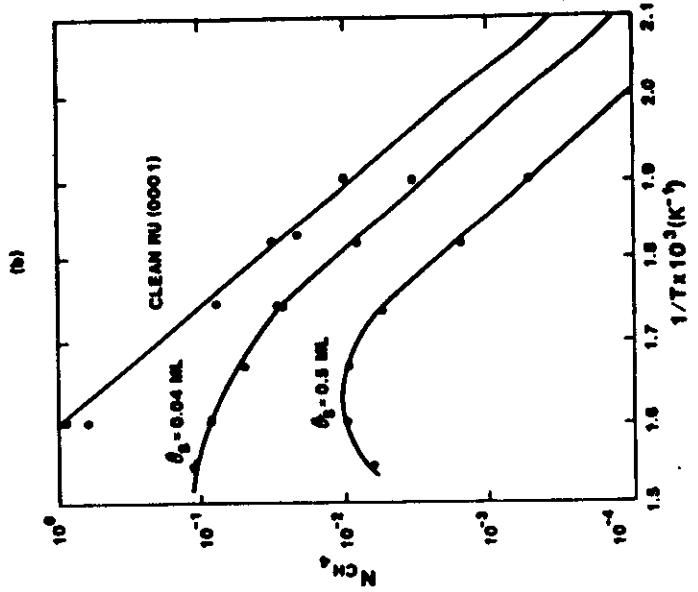
(b)
CLEAN RU (0001)
θS=0.04 ML
θS=0.5 ML
1/T x10³(K⁻¹)
NCH4

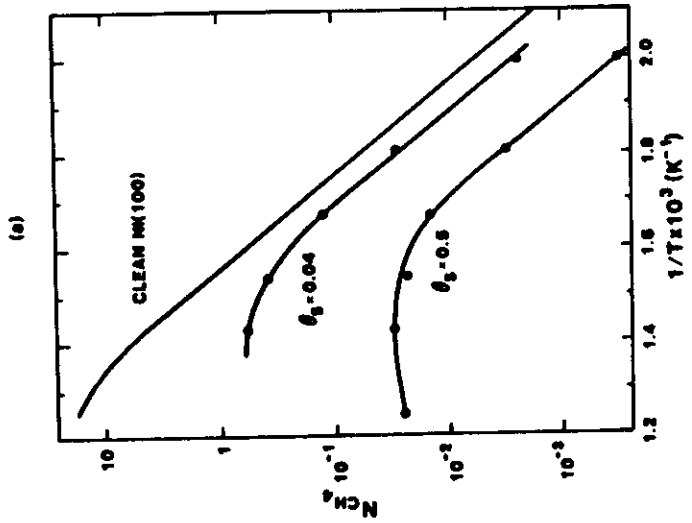
(a)
CLEAN NI(100)
θS=0.04
θS=0.5
1/T x10³ (K⁻¹)
NCH4

(3)

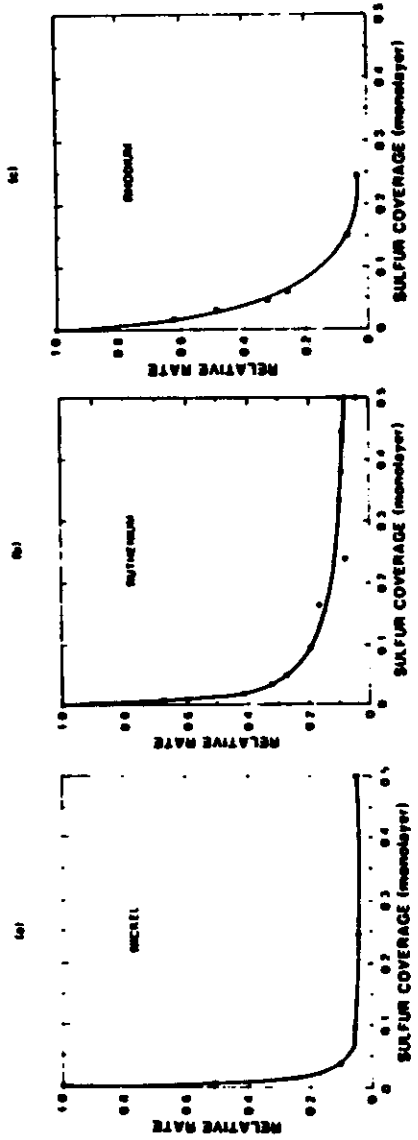
SULFUR COVERAGE (monolayer)
RELATIVE RATE

(4)

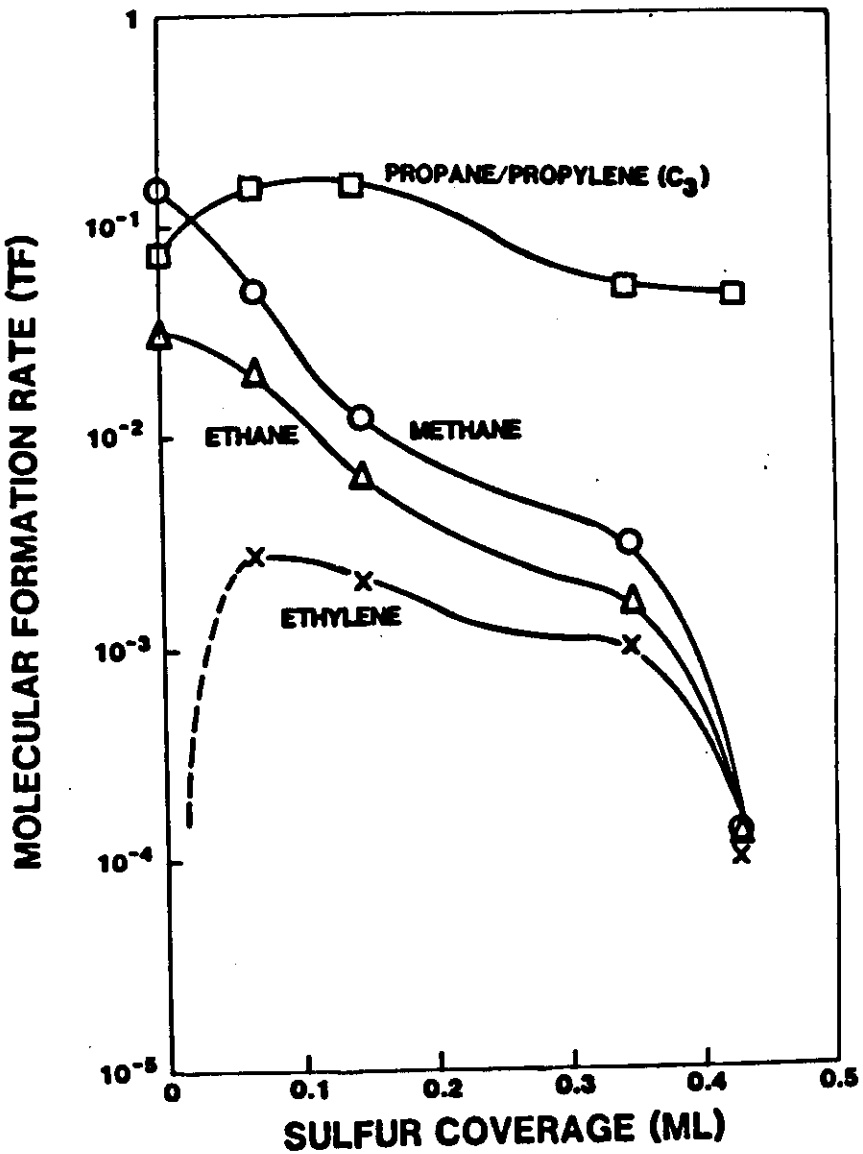
MOLECULAR FORMATION RATE (TF)
SULFUR COVERAGE (ML)
PROPANE/PROPYLENE (C_3)
METHANE
ETHANE
ETHYLENE
1
10^{-1}
10^{-2}
10^{-3}
10^{-4}
10^{-5}
0
0.1
0.2
0.3
0.4
0.5

(5)

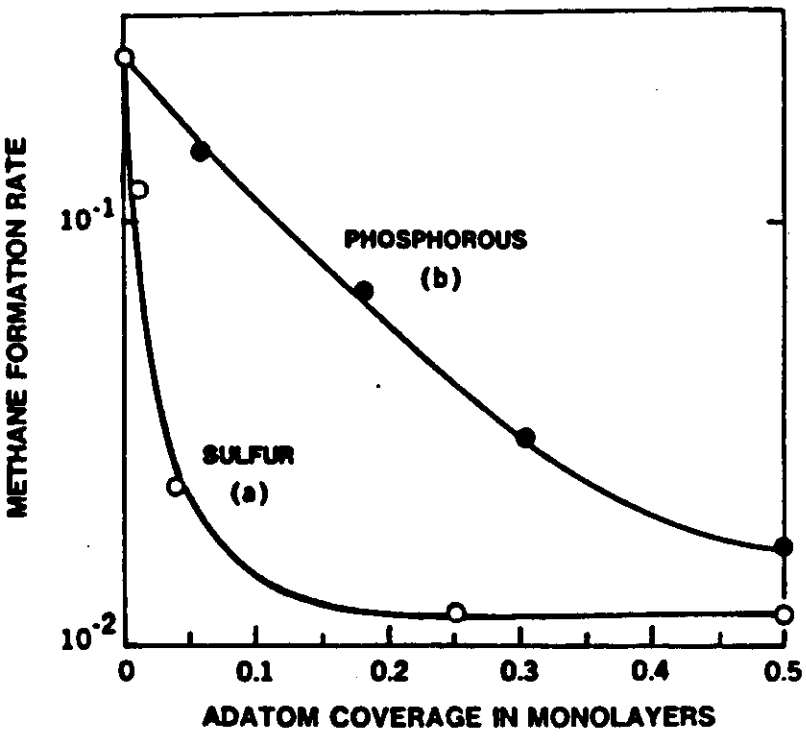
METHANE FORMATION RATE
10^{-1}
10^{-2}
PHOSPHOROUS
(b)
SULFUR
(a)
0
0.1
0.2
0.3
0.4
0.5
ADATOM COVERAGE IN MONOLAYERS

(6)

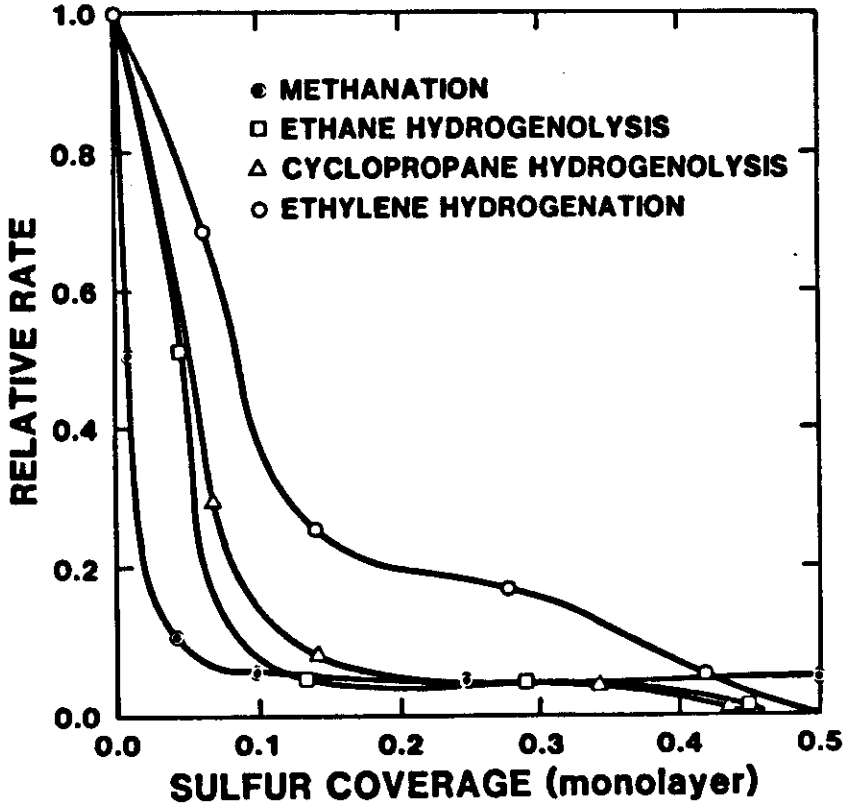
RELATIVE RATE
1.0
0.8
0.6
0.4
0.2
0.0
METHANATION
ETHANE HYDROGENOLYSIS
CYCLOPROPANE HYDROGENOLYSIS
ETHYLENE HYDROGENATION
0.0
0.1
0.2
0.3
0.4
0.5
SULFUR COVERAGE (monolayer)

(7)

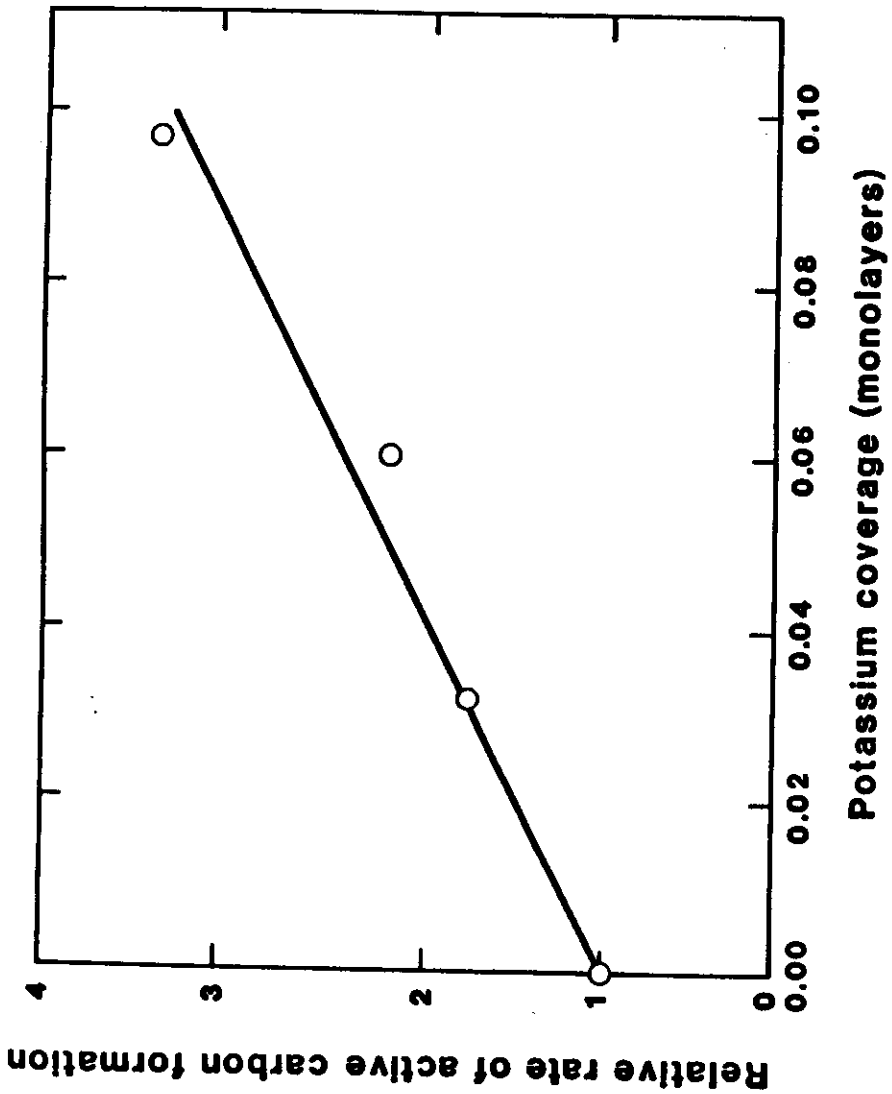
Relative rate of active carbon formation
Potassium coverage (monolayers)
0.00
0.02
0.04
0.06
0.08
0.10
0
1
2
3
4

(8)

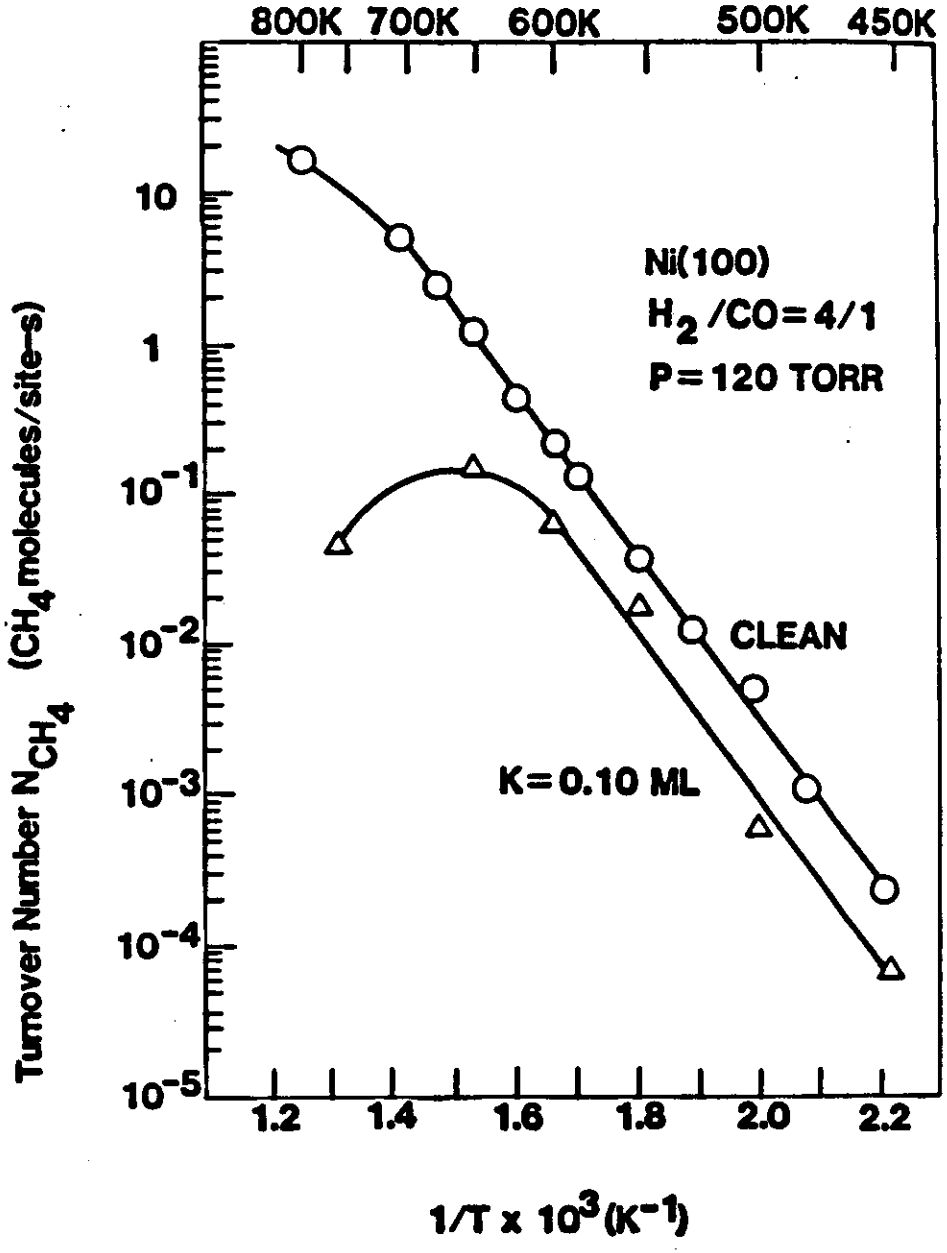
800K 700K 600K 500K 450K
Turnover Number N_{CH_4} (CH_4 molecules/site-s)
Ni(100)
H_2/CO=4/1
P=120 TORR
CLEAN
K=0.10 ML
10
1
10^{-1}
10^{-2}
10^{-3}
10^{-4}
10^{-5}
1.2
1.4
1.6
1.8
2.0
2.2
1/T x 10^3(K^{-1})

(9)

Surface Properties of Mixed-Metal Catalysts

D. W. Goodman
Surface Science Division
Sandia National Laboratories
Albuquerque, NM 87185

ABSTRACT

The chemical behavior of monolayer coverages of one metal on the surface of another, i.e., Cu/Ru, Ni/Ru, Ni/W, Fe/W, Pd/W, has recently been shown to be dramatically different from that seen for either of the metallic components separately. These chemical alterations, which modify the chemisorption and catalytic properties of the overlayers, have been correlated with changes in the structural and electronic properties of the bimetallic system. The films are found to grow in a manner which causes them to be strained with respect to their bulk lattice configuration. In addition, unique electronic interface states have been identified with these overlayers. These studies, which include the adsorption of CO and H_2 on these overlayers as well as the measurement of the elevated pressure kinetics of the methanation, ethane hydrogenolysis, cyclohexane dehydrogenation reactions, are reviewed.

In addition to modification of surfaces by non-metals, the catalytic properties of metals can also be altered greatly by the addition of a second transition metal [1]. Interest in bimetallic catalysts has risen steadily over the years because of the commercial success of these systems. This success results from an enhanced ability to control the catalytic activity and selectivity by tailoring the catalyst composition [2,3]. A long-standing question regarding such bimetallic systems is the nature of the properties of the mixed metal system which give rise to its enhanced catalytic performance relative to either of its individual metal components. These enhanced properties (improved stability, selectivity and/or activity) can be accounted for by one or more of several possibilities. First, the addition of one metal to a second may lead to an electronic modification of either or both of the metal constituents. This electronic perturbation can result from direct bonding (charge transfer) or from a structural modification induced by one metal upon the other. Secondly, a metal additive can promote a particular step in the reaction sequence and, thus, act in parallel with the host metal. Thirdly, the additive metal can serve to block the availability of certain active sites, or ensembles, prerequisite for a particular reaction step. If this "poisoned" reaction step involves an undesirable reaction product, then the net effect is an enhanced overall selectivity. Further, the attenuation by this mechanism of a reaction step leading to undesirable surface contamination will promote catalyst activity and durability.

The studies reviewed here are part of a continuing effort [7-10] to identify those properties of bimetallic systems which

can be related to their superior catalytic properties. A pivotal question to be addressed of bimetallic systems (and of surface impurities in general) is the relative importance of ensemble (steric or local) versus electronic (nonlocal or extended) effects in the modification of catalytic properties. In gathering information to address this question it has been advantageous to simplify the problem by utilizing models of a bimetallic catalyst such as the deposition of metals on single-crystal substrates in the clean environment familiar to surface science.

These studies were carried out utilizing the specialized apparatus described in references [11,12]. This device consists of two distinct regions, a surface analysis chamber and a microcatalytic reactor. The custom built reactor, contiguous to the surface analysis chamber, employs a retraction bellows that supports the metal single crystal and allows translation of the catalyst in vacuo from the reactor to the surface analysis region. Both regions are of ultrahigh vacuum construction, bakeable, and capable of ultimate pressures of less than 2×10^{-10} Torr. Auger spectroscopy (AES) is used to characterize the sample before and after reaction. A second chamber was equipped with Auger spectroscopy, low energy electron diffraction (LEED) and a mass spectrometer for temperature programmed desorption (TPD).

Many such model systems have been studied but a particularly appealing combination is that of Cu on Ru. Cu is immiscible in Ru which facilitates coverage determinations by TPD

[4] and circumvents the complication of determining the 3-d composition. The adsorption and growth of Cu films on the Ru(0001) surface have been studied [4-10,13-20] by work function function measurements, LEED, AES, and TPD. The results from recent studies [4-10] indicate that for submonolayer depositions at 100K the Cu grows in a highly dispersed mode, subsequently forming 2-d islands pseudomorphic to the Ru(0001) substrate upon annealing to 300K. Pseudomorphic growth of the copper indicates that the copper-copper bond distances are strained approximately 6% beyond the equilibrium bond distances found for bulk copper.

A comparison of CO desorption from Ru [7] from multilayer Cu (.10ML) on Ru and 1ML Cu on Ru is shown in Fig. 1. The TPD features of the 1ML Cu (peaks at 160 and 210K) on Ru are at temperatures intermediate between Ru and bulk Cu. This suggests that the monolayer Cu is electronically perturbed and that this perturbation manifests itself in the bonding of CO. An increase in the desorption temperature relative to bulk Cu indicates a stabilization of the CO on the monolayer Cu suggesting a coupling of the CO through the Cu to the Ru. The magnitude of the CO stabilization implies that the electronic modification of the Cu by the Ru is significant and should be observable with a band structure probe. Recent angular resolved photoemission studies [7] indeed show a unique interface state which is likely related to the altered CO bonding on Cu films intimate to Ru.

Figure 2 shows the results [7] of CO chemisorption on the Cu/Ru(0001) system as a function of the Cu coverage. In each case the exposure corresponds to a saturation coverage of CO. Most apparent in Figure 2 is a monotonic decrease upon addition

of Cu of the CO structure identified with Ru (peaks at 400 and 480K) and an increase of the CO structure corresponding to Cu (peaks at 160 and 210K). The buildup of a third feature at ~300K (indicated by the dashed line) is assigned to correspond to CO desorbing from the edges of Cu islands. Integration of the 200, 275, and 300K peaks provides information regarding island sizes, that is, perimeter-to-island area ratios, at various Cu coverages. For example, at θ_{Cu} = 0.66 the average island size is estimated to be approximately 50A in diameter. This island size is consistent with an estimate of the 2-d island size corresponding to this coverage of 40-60A derived from the width of the LEED beam profiles [7].

Model studies of the Cu/Ru(0001) catalyst have been carried out [8] for methanation and hydrogenolysis reactions. These data suggest that copper merely serves as an inactive diluent, blocking sites on a one-to-one basis. Similar results have been found in analogous studies [21] introducing silver onto a Rh(111) methanation catalyst.

Sinfelt [22] has shown that copper in a Cu/Ru catalyst is confined to the surface of ruthenium. Results from the model catalysts discussed here then should be relevant to those on the corresponding supported, bimetallic catalysts. Several such studies have been carried out investigating the addition of copper or other Group 1B metals on the rates of CO hydrogenation [23-25] and ethane hydrogenolysis [25] catalyzed by ruthenium. In general, these studies show a marked reduction in activity with addition of the Group 1B metal suggesting a more profound

effect of the Group 1B metal on ruthenium than implied from the model studies. A critical parameter in the supported studies is the measurement of the active ruthenium surface using hydrogen chemisorption techniques. Haller and coworkers [26,27] have recently suggested that hydrogen spillover during chemisorption may occur from ruthenium to copper complicating the assessment of surface Ru atoms. Recent studies in our laboratory [5,6] have shown directly that spillover from Ru to Cu can take place and must be considered in the hydrogen chemisorption measurements. H_2 spillover would lead to a significant overestimation of the number of active ruthenium metal sites and thus to significant error in calculating ruthenium specific activity. If this is indeed the case, the results obtained on the supported catalysts, corrected for the overestimation of surface ruthenium, could become more comparable with the model data reported here. Finally, the activation energies observed on supported catalysts in various laboratories are generally unchanged by the addition of Group 1B metal [26-28] in agreement with the model studies.

These arguments suggest that Ru specific rates for methanation and ethane hydrogenolysis on supported Cu/Ru catalysts approximate those values found for pure Ru. As a consequence, the rates for cyclohexane dehydrogenation reaction on supported Cu/Ru, similarly corrected, must exceed those specific rates found for pure Ru. The uncorrected specific rates for cyclohexane dehydrogenation on the supported Cu/Ru system remain essentially unchanged upon addition of Cu to Ru [28]. An activity enhancement for cyclohexane dehydrogenation in the mixed Cu/Ru system relative to pure Ru is most surprising given that Cu

is less active for this reaction than Ru.

Figure 3 shows the effect of the addition of Cu to Ru on the rate of cyclohexane dehydrogenation to benzene. The overall rate of this reaction is seen to increase by approximately an order of magnitude at a copper coverage of 3/4 of a monolayer. This translates to a Ru specific rate enhancement of ~40. Above this coverage, the rate falls to an activity approximately equal to that of Cu-free Ru. The observation of non-zero rates at the higher Cu coverages is believed to be caused by three dimensional clustering of the Cu overlayers [29]. Similar data have been obtained for this reaction on epitaxial and alloyed Au/Pt(111) surfaces [30].

The rate enhancement observed for submonolayer Cu deposits may relate to an enhanced activity of the strained Cu film for this reaction due to its altered geometric [29] and electronic [9] properties. Alternatively, a mechanism whereby the two metals cooperatively catalyze different steps of the reaction may account for the activity promotion. For example, dissociative H_2 adsorption on bulk Cu is unfavorable due to an activation barrier of approximately 5 kcal/mol [31]. In the combined Cu/Ru system, Ru may function as an atomic hydrogen source/sink via spillover to/from neighboring Cu. A kinetically controlled spillover of H_2 from Ru to Cu, discussed above, is consistent with an observed optimum reaction rate at an intermediate Cu coverage.

Finally, we note the differences between a Ru(0001) catalyst with or without added Cu with respect to attaining steady-state reaction rates. On the Cu-free surface, an induction time of

approximately 10 minutes is required to achieve steady state activity. During this time, production of benzene is quite low while the hydrogenolysis to lower alkanes, primarily methane, is significantly higher than at steady-state. During this induction time the carbon level (as determined by Auger spectroscopy) rises to a saturation value coincidental with the onset of steady state reaction. This behavior suggests that a carbonaceous layer on the metal surface effectively suppresses carbon-carbon bond scission, or hydrogenolysis, on the Ru surface.

Cu addition leads to an enhanced rate of benzene production with little or no induction time. That is, the initial rate of cyclohexane hydrogenolysis, relative to the Cu-free surface, is suppressed. Further, Cu reduces the relative carbon buildup on the surface during reaction. Thus, Cu may play a similar role as the carbonaceous layer in suppressing cyclohexane hydrogenolysis while concurrently stabilizing those intermediates leading to the product benzene. In addition, copper may serve to weaken the chemisorption bond of benzene and thus limit self-poisoning by adsorbed product. This latter possibility has been proposed by Sachtler and Somorjai [30] to explain the role of Au in Au/Pt(111) catalysts for this reaction. A weakening of benzene chemisorption satisfactorily accounts for our observation that the reaction changes from zero order in cyclohexane on Ru(0001) to approximately first order upon the addition of Cu.

A second bimetallic system which has been thoroughly studied is nickel adsorbed onto tungsten [32,33]. Figures 4 and 5 show plots of the AES Ni(848eV)/W(179eV) peak height ratios as a function of the Ni (Mass 58) TPD area following deposition of Ni

onto W(110) and W(100) substrates, respectively. On both surfaces Ni is adsorbed layer-by-layer with clear breaks in the AES data of Figs. 4 and 5 at each successive monolayer. Annealing Ni layers with coverages less than 1.3 ML to 1200K produced little change in the Ni(848eV)/W(179eV) AES ratio. However, for Ni coverages above 1.3ML, a 1200K anneal resulted in a very slow increase in this AES ratio with coverage, indicating either alloy or 3-dimensional island formation.

The growth of Ni layers on W(110) and (100) subsequent to the first monolayer, determined by the breaks in the AES vs. TPD area curves shown in Figs. 4 and 5, do not yield TPD areas that correspond to simple multiples of the TPD area found for the monolayer TPD feature. This result indicates that the second and successive Ni layers have significantly altered Ni atomic densities compared with the first Ni layer. On W(110) the ratio of the first to second monolayer TPD areas, 0.78, compares favorably with the ratio of the surface atomic densities of Ni(111) and W(110), 0.79, using the values 1.81×10^{15} and 1.43×10^{15} for the atomic densities of Ni(111) and W(110), respectively. On W(100) the ratio of Ni atoms in the first to the second layers, 0.52, is near the ratio of the surface atomic densities of Ni(111) and W(100), 0.55, using a value of 1.0×10^{15} for the surface atomic density of W(100). These results are consistent with pseudomorphic growth of the monolayer, with second and subsequent Ni layers relaxed to or near the Ni(111) structure. LEED results support this conclusion in that only the 1x1 pattern from either W surface is observed below the first AES

break. At higher Ni coverages satellite spots develop along the <111> direction for Ni/W(110); a complex pattern is observed above the first monolayer break for Ni/W(100). Satellite spots were observed at Ni coverages less than 1ML for an unannealed Ni overlayer; however, annealing to ~1150K (just below the onset of desorption) produced a sharp 1x1 LEED pattern. These results are consistent with some 3-dimensional island formation occurring upon Ni deposition at 100K.

The AES data of Fig 4 indicate only a single break in the region around 1ML in the plot of Ni(848eV)/W(179eV) AES ratio versus TPD area (i.e. Ni coverage). That is, no evidence is found for a double break near the 1 ML Ni coverage as reported in the work of Kolaczkiewicz and Bauer [34] for the Ni/W(110) system. The onset of the second monolayer Ni TPD peak is detected precisely at the AES break, and no change in desorption temperature for the first Ni monolayer is detected from 1.0 to 1.2 ML. Adsorption of Ni beyond the first monolayer results in the appearance of a second Ni TPD peak (see Fig. 6), and the introduction in the LEED of satellite spots, due to the presence of atoms in the second layer. Changes in the chemisorptive properties would be expected for a phase transition such as that reported by Kolaczkiewicz and Bauer [34], considering the structural and electronic modification that would accompany this transition. However, no apparent changes in the chemisorption properties of the first monolayer were observed near the atom density at which the phase transition was reported.

CO TPD data [32] as a function of Ni coverage on W(110) are shown in Fig. 6. As the Ni coverage is increased from 0.3 to

1.0ML, adsorption on the W(110) substrate decreases, as evidenced by a reduction in the CO features between 225 and 350K, while a feature at 380K becomes more prominent. The 380K CO TPD peak maximum for 1ML Ni compares with 430K for the CO TPD peak maximum for Ni(111) [35]. Increasing the Ni coverage above 1.0ML results in a broadening of the 380K CO TPD peak and in the development of a shoulder feature, suggestive of bulk Ni CO desorption, at ~430K.

CO chemisorption on the Ni/W(100) surface is similar to CO adsorption on Ni/W(110). Fig. 7 shows CO desorption as a function of Ni coverage on W(100). As the Ni coverage is increased from 0.3 to 1.0ML, decreasing intensity in the TPD features associated with W(100) are evident near 300K. At a Ni coverage of 1ML, the CO TPD peak maximum is reduced by approximately 50K from the corresponding peak maximum on Ni(100) [36]. For coverages greater than 1ML, a clear shoulder at 420-450K is observed, indicating that second and successive Ni layers have chemisorptive properties very similar to bulk Ni. Thus the W substrates clearly alter the chemisorptive properties of the first Ni layer, but have only slight effects on the second and subsequent layers.

That CO chemisorption is perturbed on strained-layer Ni is not surprising in view of CO chemisorption behavior on other metal overlayer systems. For example, on Cu/Ru it has been proposed that charge transfer from Cu to Ru results in decreased occupancy of the Cu 4s level. This electronic modification makes Cu more "nickel-like," and results in an increase in the binding

energy for CO. Similarly Cu/W [37] also exhibits charge transfer to the substrate and a increase in CO binding strength to Cu. In another case where the CO binding energy increases, Ni/Ru [38], an increase in the density of states is observed close to the Fermi level. The increased electron density may result in increased metal-CO backbonding, which in turn would increase the binding energy of CO.

In contrast to the above examples, CO on Ni/W is less strongly bound to the Ni monolayer than to bulk Ni. One explanation for this effect is that the charge transfer observed from Ni to W [34] results in a shift of the Ni d levels, relevant to CO bonding, to higher binding energies (i.e. farther from the Fermi level). Indeed, such an effect has been observed in the case of Ni/Nb(110) and Pd/Ta(110) [39]. Similarly, results on other group VIII metal - W systems [40-41] have shown a decrease in the CO binding strength.

The catalytic activity of strained layer Ni on W(110) for methanation and ethane hydrogenolysis has been studied as a function of Ni coverage [42]. The activity per Ni atom site for methanation, a structure insensitive reaction, is independent of the Ni coverage and similar to the activity found for bulk Ni. The activation energy for this reaction is lower on the strained metal overlayer, however, very likely reflecting the lower binding strength of CO on the bimetallic system.

In contrast, ethane hydrogenolysis, which is a structure sensitive reaction over bulk Ni, displayed marked structural effects on the Ni/W system [42]. We have observed that the specific rate, or rate per surface metal atom, but not the

activation energy, is a strong function of metal coverage on the Ni/W(110) surface, suggesting that the critical reaction step involves the need for a single, sterically unhindered Ni atom. On the Ni/W(100) surface the specific reaction rate was independent of Ni coverage. In addition, the rate on bulk Ni(100), Ni/W(110) in the limit of zero coverage, and Ni/W(100) were all equal, as were the activation energies. This implies that on Ni/W(100) the Ni atom geometry is sufficiently open to allow unhindered access to each Ni atom. Apparently on the Ni/W(110) surface only island edges and individual atoms display activity similar to the Ni(100) surface; the island interiors, in contrast, exhibit behavior similar to Ni(111) which has a much lower specific rate and higher activation energy. As the Ni coverage is reduced, the number of active, Ni(100)-like atoms increases, leading to an increase in the specific rate. The activation energy, however, remains unchanged.

We have studied several other metal overlayers on W(110), W(100), and Ru(0001) substrates [43]. Table 1 lists properties of the metal overlayers, and the effect of the substrate on CO chemisorption. In general only the first monolayer grows pseudomorphically, though more than one monolayer may be stable before three dimensional islands are formed (e. g. Cu/Ru grows two stable layers). The binding strength of CO is always altered from the bulk metal, though the magnitude of the effect is seemingly more dependent on the metal overlayer, than on the degree of strain induced by the substrate (represented as the atom density mismatch). As with Ni/W and Cu/Ru, the effect on CO

binding energy extends primarily to only the first monolayer; subsequent layers exhibit behavior close to the bulk metal.

ACKNOWLEDGEMENT

We acknowledge with pleasure the partial support of this work by the Department of Energy, Office of Basic Energy Sciences, Division of Chemical Sciences.

REFERENCES

1. T. B. Grimley and M. Torrini, J. Phys. Chem., 87, 4378 (1973).

2. J. H. Sinfelt, "Bimetallic Catalysts: Discoveries, Concepts, and Applications", John Wiley & Sons, NY, NY, 1983.

3. G. M. Schwab, Disc. Faraday Soc. 8, 166 (1950).

4. J. T. Yates, Jr., C. H. F. Peden, and D. W. Goodman, J. Catal., 94, 576 (1985).

5. D. W. Goodman, J. T. Yates, Jr., and C. H. F. Peden, Surf. Sci., 164, 417 (1985).

6. D. W. Goodman and C. H. F. Peden, J. Catal., 95, 321 (1985).

7. J. E. Houston, C. H. F. Peden, D. S. Blair, and D. W. Goodman, 167, 427 (1986).

8. J. E. Houston, C. H. F. Peden, P. J. Feibelman, and D. W. Goodman, I&EC Fundamentals, 25, 58 (1986).

9. J. E. Houston, C. H. F. Peden, P. J. Feibelman, and D. R. Hamann, Phys. Rev. Lett., 56, 375 (1986).

10. C. H. F. Peden and D. W. Goodman, J. Catal., 104, 347 (1987).

11. D. W. Goodman, R. D. Kelley, T. E. Madey, and J. T. Yates, Jr., J. Catal. 64, 479 (1980).

12. D. W. Goodman, Ann. Rev. Phys. Chem., 37 (1986) 425; D. W. Goodman, Accts. Chem. Res., 17, 194 (1984); D. W. Goodman, J. Vac. Sci. Tech., 20, 522 (1982).

13. H. Shimizu, K. Christmann and G. Ertl, J. Catal., 61, 412 (1980).

14. J. C. Vickerman, K. Christmann and G. Ertl, J. Catal., 71, 175 (1981).

15. S. K. Shi, H. I. Lee and J. M. White, Surf. Sci., 102, 56 (1981).

16. L. Richter, S. D. Bader and M. B. Brodsky, J. Vac. Sci. Techn., 18, 578 (1981).

17. J. C. Vickerman and K. Christmann, Surf. Sci., 120, 1 (1982).

18. J. C. Vickerman, K. Christmann, G. Ertl, P. Heiman, F. J. Himpsel, and D. E. Eastman, Surf. Sci., 134, 367 (1983).

19. S. D. Bader and L. Richter, J. Vac. Sci. Technol., A1, 1185 (1983).

20. C. Park, E. Bauer, And H. Poppa, Surf. Sci., submitted for publication.

21. D. W. Goodman in "Heterogeneous Catalysis" (Proceedings of IUCCP Conference), Texas A&M University, 1984.

22. J. H. Sinfelt, G. H. Via, and F. W. Lytle, Catal. Rev.-Sci. Eng., 26, 81 (1984).

23. A. K. Datye and J. Schwank, J. Catal., 93, 256 (1985).

26. A. J. Rouco, G. L. Haller, J. A. Oliver, and C. Kemball, J. Catal., 84, 297 (1983).

27. G. L. Haller, D. E. Resasco, and J. Wang, J. Catal., 84, 477 (1983).

28. J. H. Sinfelt, J. Catal., 29, 308 (1973).

29. J. E. Houston, C. H. F. Peden, D. S. Blair and D. W. Goodman, Surface Sci., 167, 427 (1986).

30. Sachtler, J.W.A. and Somorjai, G.A., J. Catal. 89, 35 (1984).

31. Balooch, M., Cardillo, M.J., Miller, D.R., and Stickney, R.E., Surf. Sci. 50, 263 (1975).

24. G. C. Bond and B. D. Turnham, J. Catal., 45, 128 (1976).

25. L. J. M. Luyten, M. v. Eck, J. v. Grondelle, and J. H. C. v. Hooff, J. Phys. Chem., 82, 2000 (1978).

32. P.J. Berlowitz and D.W. Goodman, Surf. Sci. 187, 463 (1987).

33. M. Balooch, M.J. Cardillo, D.R. Miller, R.E. Stickney, Surf. Sci. 50, 263 (1975).

34. J. Kolaczkiewicz and E. Bauer, Surf. Sci. 144, 495 (1984).

35. K. Christmann, O. Schober, G. Ertl, J. Chem. Phys. 60, (1974).

36. D.W. Goodman, J.T. Yates, Jr., T.E. Madey, Surf. Sci. 93, L135 (1980).

37. I. Hamedeh and R. Gomer, Surf. Sci. 154, 168 (1985).

38. J.E. Houston, J.M. White, P.J. Berlowitz, D. W. Goodman, Surface Sci., in press.

39. M.W. Ruckman, M. Strongin, X. Pan, ibid.

40. D. Prigge, W. Schlenk, E. Bauer, Surf. Sci. 123, L698

(1982).

41. R.W. Judd, M.A. Reichelt, R.M. Lambert (to be submitted for publication).

42. C.H.F. Peden and D.W. Goodman, J. Catal. 100, 5209 (1986).

43. P. J. Berlowitz, C. H. F. Peden, and D. W. Goodman, Mat. Res. Soc. Symp. Proc., 83, 161 (1987).

FIGURE CAPTIONS

Figure 1. TPD results for CO adsorbed to saturation levels on clean Ru(0001), on multilayer Cu, and on a 1ML Cu covered Ru(0001). (From ref. [7])

Figure 2. TPD results corresponding to CO adsorbed to saturation levels on the clean Ru(0001) surface, and from this same surface containing various coverages of Cu. (From ref. [7])

Figure 3. Relative rate of reaction versus surface Cu coverage on Ru(0001) for cyclohexane dehydrogenation to benzene. P_T = 101 Torr. H_2/cyclohexane = 100. T = 650K. (From ref. [29])

Figure 4. Adsorption of Ni on W(110) plotted as the ratio Ni(848):W(179) Auger transitions versus Ni desorbed in TPD. Ni deposition was carried out at 100K. (From ref. [32])

Figure 5. Adsorption of Ni on W(100) plotted as the ratio of Ni(848):W(179) Auger transitions versus Ni desorbed in TPD. Ni deposition was carried out at 100K. (From ref. [32])

Figure 6. TPD of CO vs. Ni coverage on W(110) for an exposure of approximately 2L at 100K. (From ref. [32])

Figure 7. TPD of CO vs. Ni coverage on W(100) for an exposure of approximately 2L at 100K. (From ref. [32])

Table 1. Comparison of Strained-Metal Overlayer Systems

Adsorbate	Substrate	Atom Density Mismatch/ML	Pseudomorphic/Epitaxial Layers	Change in CO Desorption T
Cu	Ru(0001)	6%	1/2	50K
Cu	W(110)	20	1/1	80
Ni	W(110)	21	1/1	-50
Ni	W(100)	42	1/1	-50
Ni	Ru(0001)	15	1/1	50
Pd	W(110)	10	1/1	-200
Pd	W(100)	35	2/2	-170
Pd	Ta(110)	18	1/1	-230
Fe	W(110)	9	1/2	-50
Fe	W(100)	35	2/2	-60

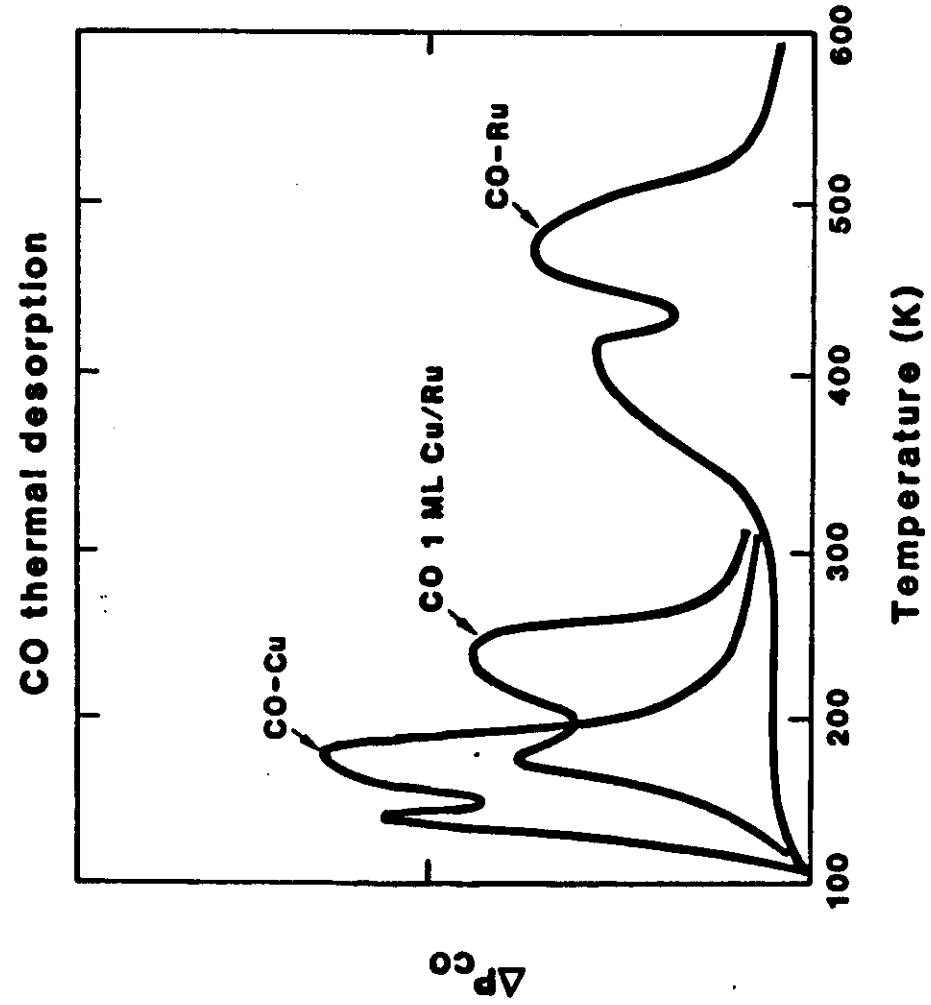

(1)

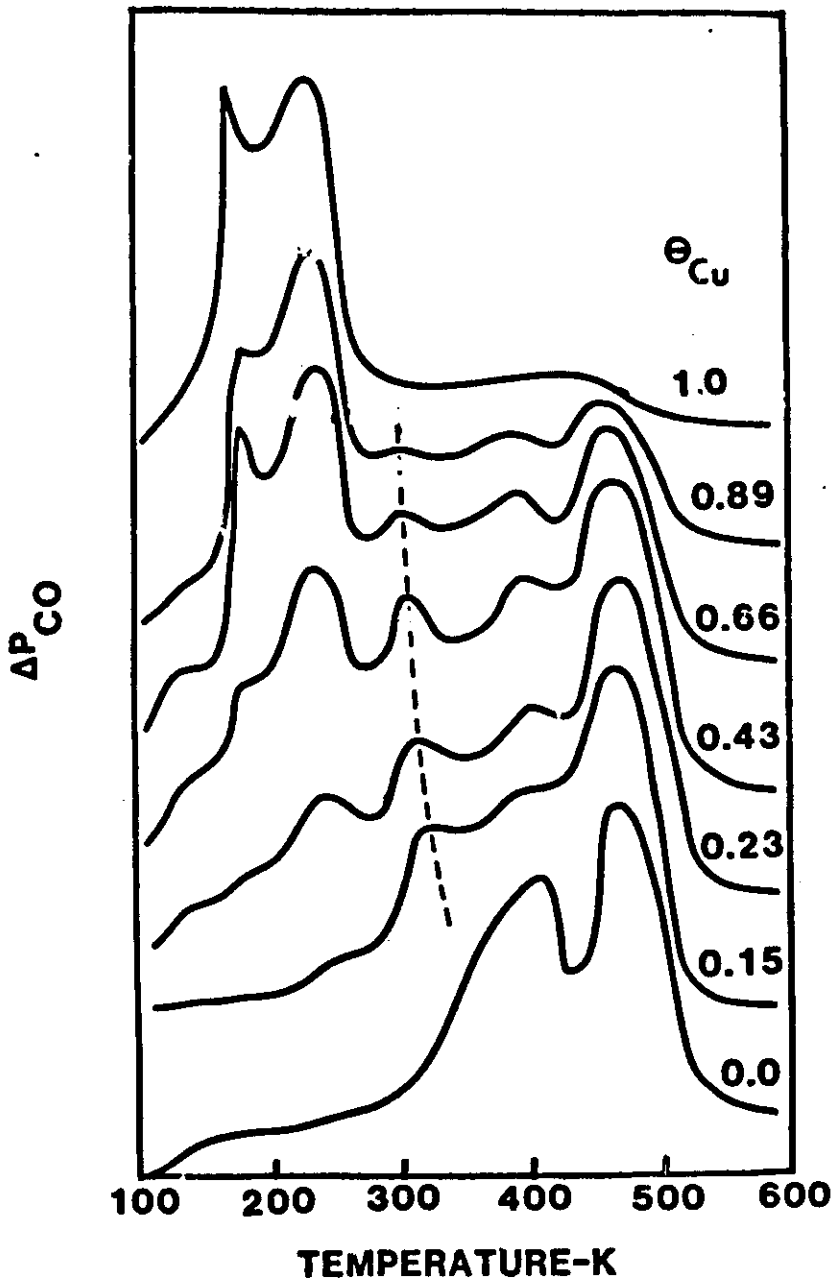
ΔP_{CO}
Θ_{Cu}
1.0
0.89
0.66
0.43
0.23
0.15
0.0
100
200
300
400
500
600
TEMPERATURE-K

(2)

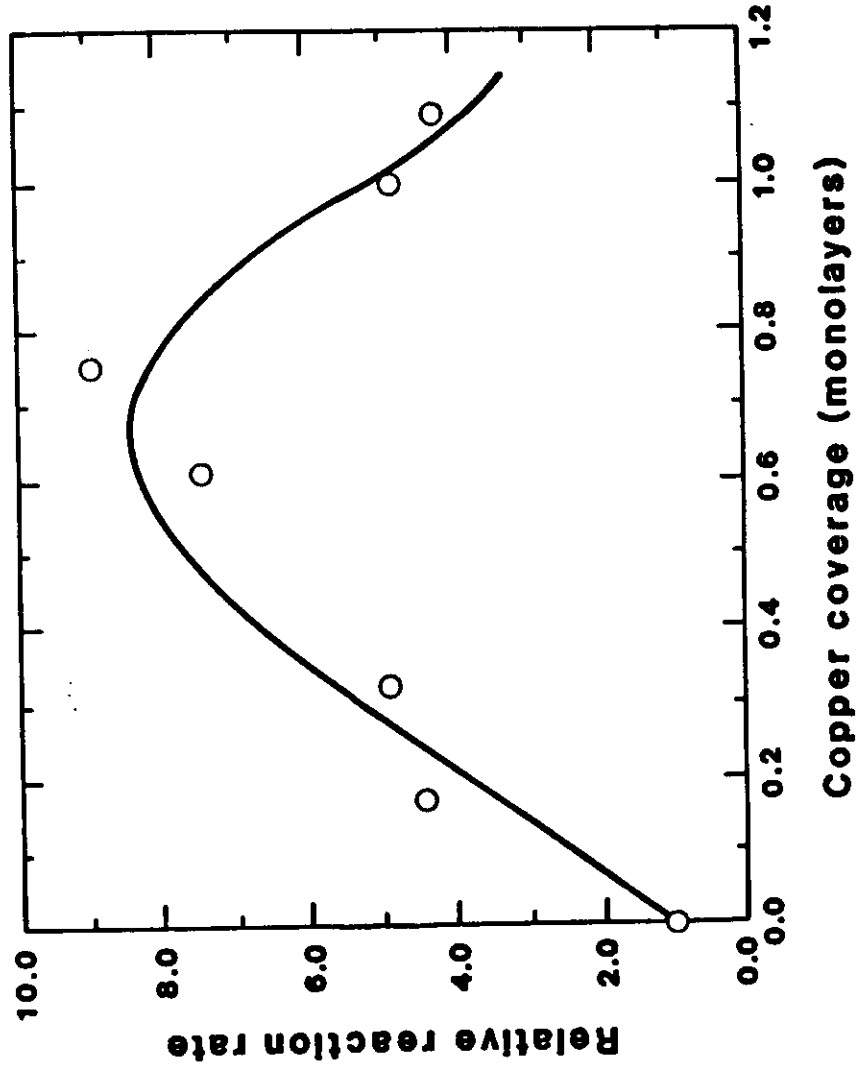
Relative reaction rate
10.0
8.0
6.0
4.0
2.0
0.0
Copper coverage (monolayers)
0.0
0.2
0.4
0.6
0.8
1.0
1.2

(3)

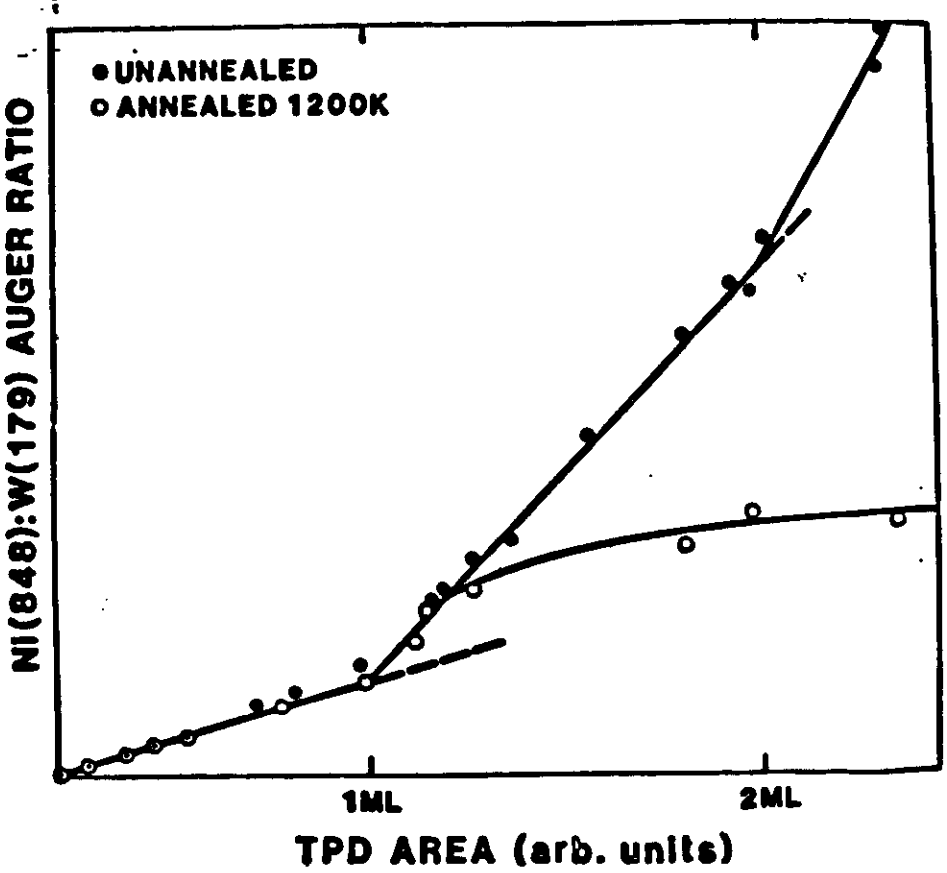
● UNANNEALED
○ ANNEALED 1200K
NI(848):W(179) AUGER RATIO
1ML
2ML
TPD AREA (arb. units)

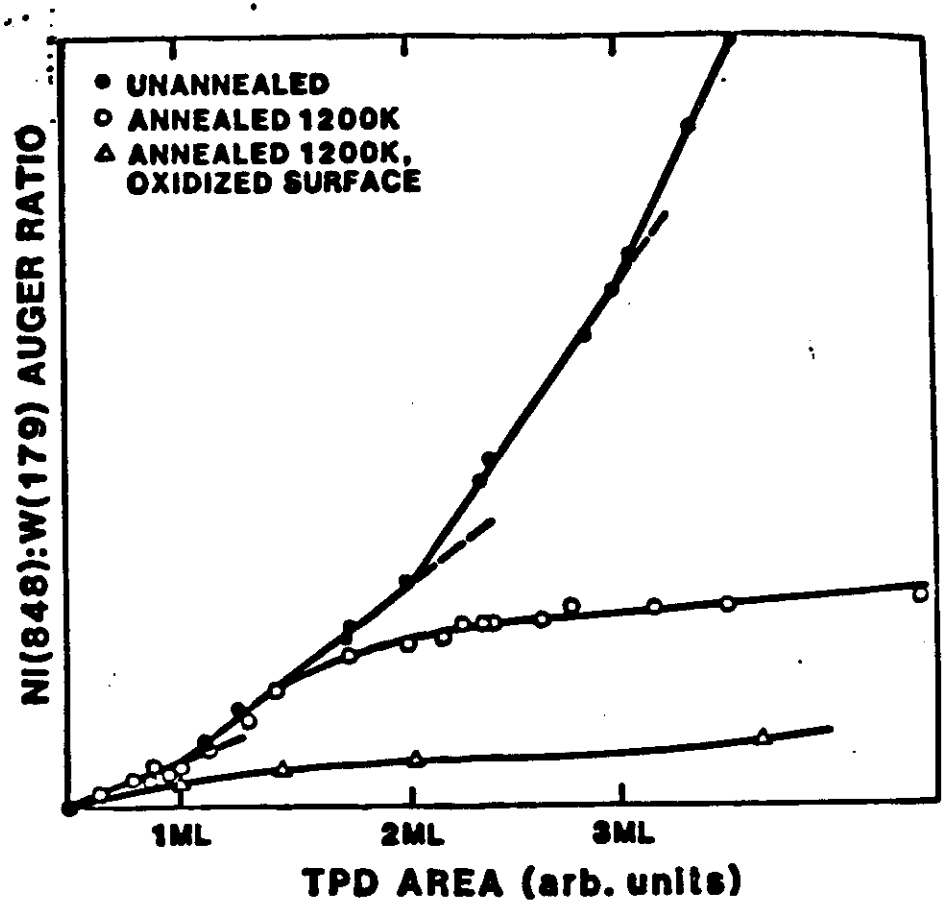
● UNANNEALED
○ ANNEALED 1200K
△ ANNEALED 1200K, OXIDIZED SURFACE
NI(848):W(179) AUGER RATIO
1ML
2ML
3ML
TPD AREA (arb. units)

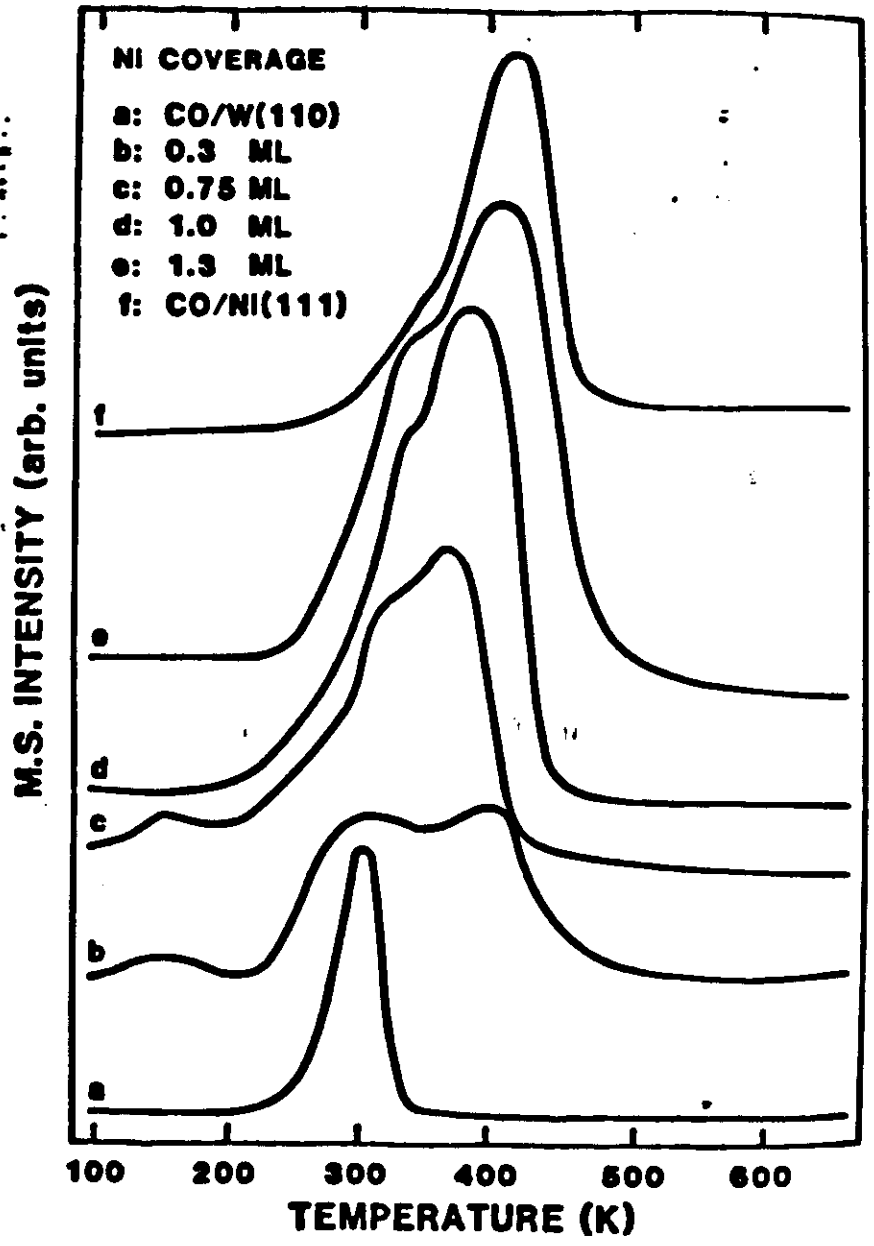
NI COVERAGE
a: CO/W(110)
b: 0.3 ML
c: 0.75 ML
d: 1.0 ML
e: 1.3 ML
f: CO/NI(111)
M.S. INTENSITY (arb. units)
100
200
300
400
500
600
TEMPERATURE (K)

(6)

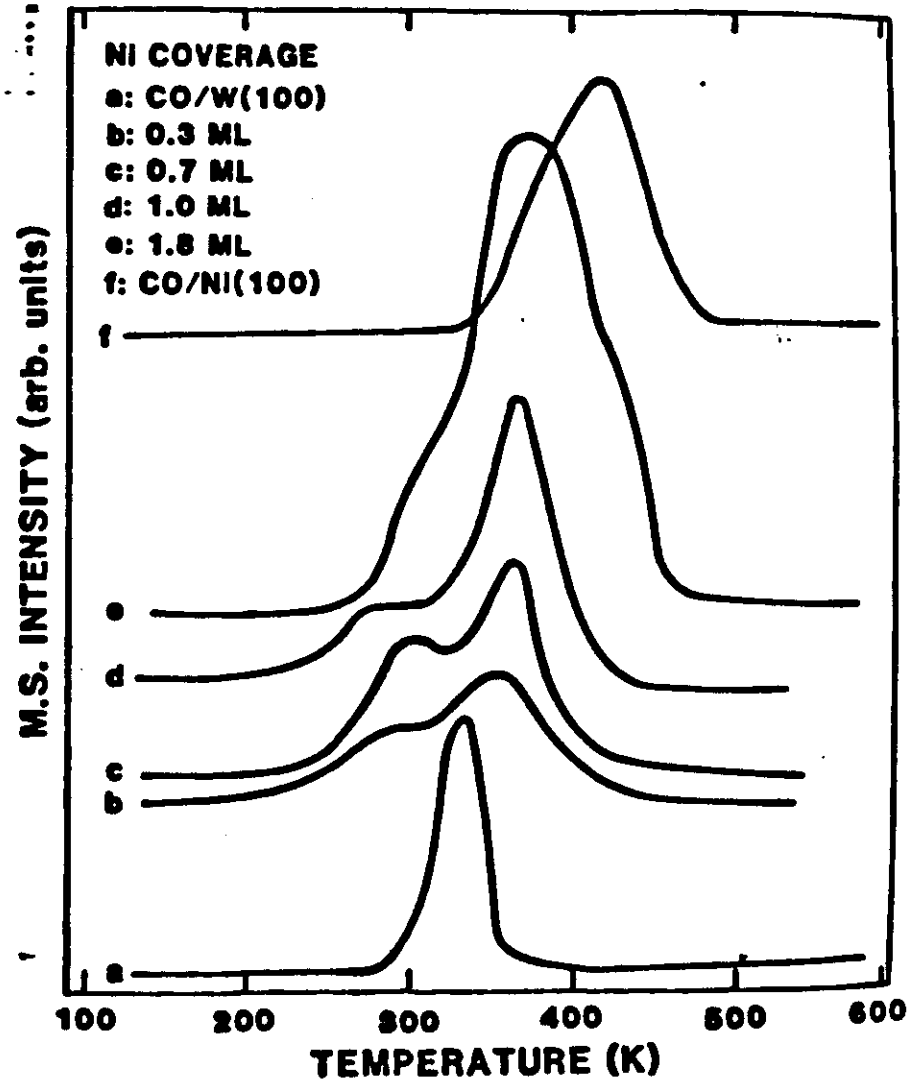
NI COVERAGE
a: CO/W(100)
b: 0.3 ML
c: 0.7 ML
d: 1.0 ML
e: 1.8 ML
f: CO/NI(100)
M.S. INTENSITY (arb. units)
100
200
300
400
500
600
TEMPERATURE (K)

(7)